Journal of Materials Chemistry C

Tuning Electronic Properties in $LaNiO_3$ Thin Films by B-site Cu-substitution

Journal:	*Journal of Materials Chemistry C*
Manuscript ID	TC-ART-07-2020-003406.R1
Article Type:	Paper
Date Submitted by the Author:	18-Aug-2020
Complete List of Authors:	Sønsteby, Henrik; University of Oslo, Chemistry Skaar, Erik; University of Oslo, Chemistry Bratvold, Jon; University of Oslo, Chemistry Freeland, John; Argonne National Laboratory Yanguas-Gil, Angel; Argonne National Laboratory Elam, Jeffrey; Argonne National Laboratory, Energy Systems Division Nilsen, Ola; University of Oslo, Department of Chemistry Fjellvåg, Helmer; University of Oslo, Chemistry

ARTICLE

Tuning Electronic Properties in $LaNiO_3$ Thin Films by B-site Cu-substitution

Received 00th January 20xx,
Accepted 00th January 20xx

DOI: 10.1039/x0xx00000x

Henrik H. Sønsteby*[a,b], Erik Skaar[a], Jon E. Bratvold[a], John W. Freeland[b], Angel Yanguas-Gil[b], Jeffrey W. Elam[b], Ola Nilsen[a] and Helmer Fjellvåg*[a]

Resistors are essential parts of futuristic all-oxide electronic architectures, yet easily overlooked due to their apparent simplicity. Herein, design of thin films with specific resistance spanning six orders of magnitude by partial substitution of Cu^{2+} for Ni^{3+} in the metallic conductor $LaNiO_3$ is shown. Substitution is attainable across the whole composition range using atomic layer deposition on $LaAlO_3$ $(100)_{pc}$ substrates, however with some inclusion of Ruddlesden-Popper RP1 phase (La_2CuO_4) at high levels of Cu-incorporation. The thermal stability of the resistance is based on a metal-insulator transition that evolves from non-existent for $LaNiO_3$ to above room-temperature for high Cu^{2+} substitution. This provides further insight in the metal-insulator transition found for correlated rare-earth nickelates, especially the type of transition seen for ultrathin films of $LaNiO_3$ that is usually attributed to oxygen vacancy formation. Materials with variable resistivity and metal-insulator-transition temperatures are key in the design of futuristic electronics such as metal-insulator-transition-driven neuromorphic devices.

Introduction

Complex oxide thin films attract high interest for use in novel electronic applications.[1] Multifunctional heterostructures with combinations of functionalities allow for the design and utilization of otherwise exotic phenomena. Inherent properties can be tuned by strain engineering, sometimes resulting in surprising emergent properties at complex oxide interfaces.[2-4] This can be due to strain, electronic changes across polar discontinuities or charge transfer effects. The entirety of these effects opens for electronic devices with completely different switching mechanisms compared to traditional silicon technology. A required key component in all-complex oxide electronic devices is compounds with metallic behavior, preferably with tunable electrical resistivity. Variable resistance components find use in current limiters, voltage dividers and in all RC-circuits, as the resistance determines the rate at which a capacitor is charged.

A family of compounds that has been in the spotlight in recent years is the rare earth nickelates; $RENiO_3$ (RE = La, Pr, Nd, Sm, Eu, Gd, Tb, Dy, Ho, Er, Tm, Yb, Lu). This series of compounds is interesting due to its trend in metal-insulator transition (MIT) temperatures.[5-8] La^{3+}, the largest of the cations in this series, forms a nickelate with a rhombohedral perovskite structure (*R-3c*) that is metallic at all temperatures.[9] As the size of the rare-earth cation decreases across the series, the Ni-O-Ni bond angle decreases, resulting in a reduced *p-d*-orbital overlap and stabilization of an insulating ground state.[10] This effectively narrows the bandwidth, causing the transition to the metallic state to take place at increasing temperatures.[11] As an example, $PrNiO_3$ with a Ni-O-Ni bond angle of 158.7° has an MIT at ~140 K, accompanied by a transition from a high temperature orthorhombic (*Pnma*) metallic structure, to a low-temperature monoclinic ($P2_1/n$) insulating structure. $LuNiO_3$, with a sharp bond angle of just 143.4° has an MIT at ~600 K, accompanied by a similar structural transition. Certain solid solution rare-earth nickelates, e.g. $Nd_{0.5}Sm_{0.5}NiO_3$, exhibit an MIT very close to room temperature (i.e. in between the MIT temperatures of $NdNiO_3$ and $SmNiO_3$).

The appealing trend in MIT temperatures for A-site substitution has led to a surge of studies on the electronic behavior of $RENiO_3$, which has been thoroughly reviewed.[12] Such trends are less developed with respect to B-site substitution. The neighboring *3d* elements such as iron (Fe), cobalt (Co) and manganese (Mn) may also take +III valency, however, these ternary $RE(Mn,Co,Fe)O_3$ compounds are insulators.[13] For $LaMnO_3$, a strong Jahn-Teller distortion opens a band gap as a result of the high spin d^4 electron configuration. For $LaFeO_3$, the top of the valence band is dominated by oxygen *p*-states, while the conduction band bottom is dominated by iron *d*-states, leading to a poor overlap and a *p-d*-character band gap. For $LaCoO_3$, the band gap is a result of ligand field splitting between the different *d*-orbital bands.

[a] Department of Chemistry, Centre for Materials Science and Nanotechnology, University of Oslo, Blindern, N-0315 Oslo, Norway.
[b] Argonne National Laboratory, Lemont, Illinois 60439, USA
* henrik.sonsteby@kjemi.uio.no, helmer.fjellvag@kjemi.uio.no

Electronic Supplementary Information (ESI) available: [Extended information of quaternary composition model and detailed temperature dependent resistivity plots for determining MIT. See DOI: 10.1039/x0xx00000x

Significant work has been put into understanding the structure of the B-site solid solutions; $LaNi_{1-x}M_xO_3$ (M = Mn, Fe, Co). Rao *et al.* identified a transition to a semiconducting state in $LaNi_{1-x}Fe_xO_3$ for $x > 0.2$, explaining this with a decrease in *d*-electron itinerancy.[14] Ganguly *et al.* thereafter identified a critical substitution level, x_c, for M = Fe, Co and Mn, at which the $LaNiO_3$ host loses its metallic properties.[13] This was explained by disorder effects, and is accompanied by a transformation from rhombohedral to orthorhombic structures.

Very few studies have been carried out on intentionally substituting Ni with an element that typically takes a lower oxidation state, *e.g.* 2+. This would expectedly lead to oxygen vacancy formation. It is well known that such vacancies in a phase like *e.g.* $LaNi_{1-x}M^{(II)}{}_xO_{3-x/2}$ at some point becomes detrimental to electron conduction. This is seen also for $LaNiO_3$ with partial reduction, in the bulk phase to e.g. $La_2Ni_2O_5$, or as encountered in ultrathin films of $LaNiO_{3-x}$.[15,16] This vacancy formation appears to be more tunable and less dramatic than the abrupt transitions seen for $LaNi_{1-x}M_xO_3$ (M = Mn, Fe, Co). One viable candidate for such substitution is Cu^{2+}. First of all, it is known that oxygen deficient $LaCuO_{2.5}$ is an orthorhombic insulator.[17] Furthermore, Cu^{2+} is significantly larger than Ni^{3+}, and this may alter the Ni(Cu)-O-Ni(Cu) bond angle much in the same way as for rare-earth A-site substitution. In addition, the oxygen vacancies formed will lower the d-electron band itinerancy, narrowing the bands, and possibly open up a band gap at a set temperature. It is possible to achieve copper in +III oxidation state by applying high oxygen partial pressures, much higher than what is needed for Ni^{3+}. Under the appropriate temperature – pO_2 conditions, it ought to be possible to form $LaNi_{1-x}Cu_xO_{3-x/2}$, with Ni^{3+} and Cu^{2+} at the B-sites.

The electric properties of Cu-substituted $LaNiO_3$ is earlier just briefly described, and then only at low substitution levels. Álvarez *et al.* studied MIT temperatures in bulk $LaNi_{0.95}M_{0.05}O_{3-x}$ for M = Mo, W, Sb, Ti, Cu and Zn, synthesized using the sol-gel method based on nitrates.[18] Samples with nominal composition $LaNi_{0.95}Cu_{0.05}O_{2.96}$ exhibited a range with constant resistivity below 50 K, but no stringent MIT was observed. $LaNi_{1-x}Cu_xO_{3-\delta}$ ($0 \le x \le 1$) have also been explored, however, primarily for catalytic performance in dry methane reforming without mention of electronic transport properties.[19] An interesting observation in this study is the formation of the Ruddlesden-Popper RP1 ("214") La_2CuO_4 phase after calcination of samples with high Cu-levels (> 80 %). The superior stability of the RP1 phase may interfere with electronic transport studies for high levels of Cu substitution.[20]

No reports are found in literature on Cu-substitution of $LaNiO_3$ *thin films*. Epitaxial quaternary (pseudoternary) thin films may offer wider substitution levels than bulk samples, without decomposing to binary and ternary oxides, with intrinsic strain levels that far surpasses what can be found in bulk systems. We have previously reported on deposition of $LaNiO_3$ and $LaCuO_x$ with strong phase control by means of atomic layer deposition (ALD), using $La(thd)_3$, $Ni(acac)_2$ and $Cu(acac)_2$ as cation sources.[20,21] Ozone is used as the oxygen source. We found that $LaNiO_3$ grows epitaxial as-deposited on $LaAlO_3$ $(100)_{pc}$ and $SrTiO_3$ (100) substrates at 225 °C, with no post-annealing required to obtain the highly regarded metallic properties. $LaCuO_x$ and La_2CuO_4 are amorphous as-deposited, however, these can be crystallized into insulating $LaCuO_{2.5}$ and La_2CuO_4 upon annealing in air at 650 °C. In these oxides, we note that copper nominally is +II, however, more oxidized variants can be obtained by post-annealing in oxygen at 900 °C.[20]

In the current study, we combine the ALD processes for $LaNiO_3$ and $LaCuO_x$ in order to obtain $LaNi_{1-x}Cu_xO_{3-\delta}$ thin films across the entire x-range; $0 \le x \le 1$, at conditions that stabilizes Ni^{3+} and Cu^{2+}. We report on the structural and electric properties of such films on $LaAlO_3$ $(100)_{pc}$ substrates, and show how the resistivity and MIT temperature evolve with increased Cu-substitution. We discuss the underlying electronic mechanisms that govern conduction and the band gap opening that causes the MIT, with the main focus on the crystalline quality of the films and the level of oxygen vacancies. We finally demonstrate that the obtained films can controllably cover six orders of magnitude in resistivity at ambient conditions, with a high degree of tunability. We stress that such materials are attractive in the toolbox for the future development of all-oxide electronic devices and in monolithic integration in current device architectures.

Experimental

Thin films were deposited in an F-120 Sat ALD reactor (ASM Microchemistry) employing a chamber temperature of 225 °C under a base pressure of 2.4 mbar. The base pressure was maintained by a 300 cm^3 min^{-1} primary flow rate of N_2, supplied from gas cylinders (99.999 %) and run through a Mykrolis purifier to remove O_2 and H_2O.

$La(thd)_3$ (thd = 2,2,6,6-tetramethylheptadionato, 99%, Volatech), $Ni(acac)_2$ (acac = acetylacetonato, 99 %, Sigma Aldrich) and $Cu(acac)_2$ (99 %, Sigma Aldrich) were used as cation precursors, while O_3 was used as the oxygen source. The cation precursors were kept in open boats inside the reactor at 185, 185 and 140 °C for $La(thd)_3$, $Ni(acac)_2$ and $Cu(acac)_2$, respectively. $Ni(acac)_2$ and $Cu(acac)_2$ were resublimated in a cold-finger sublimation setup before use to enhance purity. O_3 was supplied from an AC-2505 ozone generator (In USA) fed with O_2 from gas bottles (99.5 %, Praxair) yielding 15 wt% O_3 in O_2.

Pulse durations were 2, 2, 2 and 4 seconds for $La(thd)_3$, $Ni(acac)_2$, $Cu(acac)_2$ and O_3, respectively. Purge durations were 2 seconds after cation pulses and 3 seconds after ozone pulses. This pulse and purge scheme is based on experience achieving self-limiting growth with the same precursors for deposition of the ternary component materials in the same ALD reactor throughout our prior studies.[20,21] We targeted a film thickness of 30 nm for straightforward analysis of composition and electrical properties. Samples were deposited on 1 x 1 cm^2

$LaAlO_3$ (100) single crystal substrates (Crystal GmbH) to facilitate epitaxial growth.

Routine measurements of thickness were carried out using an alpha-SE spectroscopic ellipsometer (J. A. Woollam) in the 390 – 900 nm wavelength range. A Cauchy function was employed to model the collected data.

Chemical composition was analyzed using an Axios Max Minerals x-ray fluorescence (XRF) system (Panalytical), equipped with a 4 kW Rh-tube. The system is run using Omnian and Stratos options for standardless measurement of thin films. XRF measurements were carried out on Si (100)|SiO_x substrates placed close to $LaAlO_3$ (100), to avoid any signals from substrate La during measurements.

Home-lab XRD-experiments for structural analysis was carried out on an AXS D8 Discover (Bruker) diffractometer, equipped with a LynxEye detector and a Ge (111) focusing monochromator, providing $CuK\alpha_1$ (λ = 1.5406 Å) radiation.

Room-temperature resistivity measurements were carried out using a 4-point probe and a Keithley model 2400 SourceMeter. The sheet resistivity was recorded by measuring at 10 points using currents in the range of 1 to 10 µA. Variable temperature resistivity measurements were performed on a Model 4000 physical property measurement system (PPMS; Quantum Design). The samples were mounted on a puck and contacted with gold wires on gold pads deposited by evaporation. Resistivity was collected in a 4-point setup, while the temperature was swept from 300 to 8 K.

Soft x-ray absorption spectra were collected at beamline 4-ID-C of the Argonne National Laboratory Advanced Photon Source (Lemont, IL, USA). The spectra were collected using partial fluorescence yield mode, with a resolution of 100 meV at the Ni and Cu edges. The spectra were collected at room-temperature under UHV conditions. Energy calibration was achieved by simultaneous measurement of a NiO standard with peak position at 852 eV.

Results and discussion

ALD of compounds containing more than one cation is traditionally carried out by combining processes for the binary oxide constituents. [22-24] Recipes have been developed for a range of ternary compounds, and also for some four and five component systems. This approach introduces an element of uncertainty, as the growth of a binary oxide can be strongly affected by preceding growth cycles. The traditional approach for estimating the cation stoichiometry in multicomponent oxides, developed by Nilsen *et al.*, utilizes the differences in growth per cycle (GPC) of the binary oxide constituents.[25,26] This estimate often works well for ternary systems, especially when the precursor chemistry for the different cations are similar. However, when this model is carried over to a four- or five component system, and in particular when the precursors have different ligands, the predicted values tend to deviate considerably from experimental data. To circumvent this challenge, we here introduce an alternate model for the relationship between pulsed and deposited ratios, by combining two ternary compound processes to specify the process conditions for the four-component system. The model utilizes the total growth per cycle (GPC) and absolute composition of the subset of ternary systems that form the quaternary process. In principle, one deposition of ternary compound A-B-O and one deposition of ternary compound A-C-O is sufficient to estimate the growth behavior of the quaternary process (see Supporting Information for details).

In the study of the La-Ni-Cu-O-system, we simply substitute $Ni(acac)_2$ with $Cu(acac)_2$ in the recipe for deposition of $LaNiO_3$ [5 ($La(thd)_3$ + O_3) + 2 ($Ni(acac)_2$ + O_3)].[20] The obtained films show in a relatively smooth compositional variation, as targeted and confirmed by XRF (Figure 1).

We note a good agreement between the estimated composition based on the ternary combination method and the actual deposited content. Since these films are deposited using 142 supercycles of 5 ($La(thd)_3$ + O_3) + 2 ($Ni/Cu(acac)_2$ + O_3), the effective resolution in the level of substitution is ≈ 0.4 %. The deposited cation concentration depends purely on the Cu:Ni pulsed ratio, since the $La(thd)_3$ pulsed concentration remains unchanged (Figure 2).

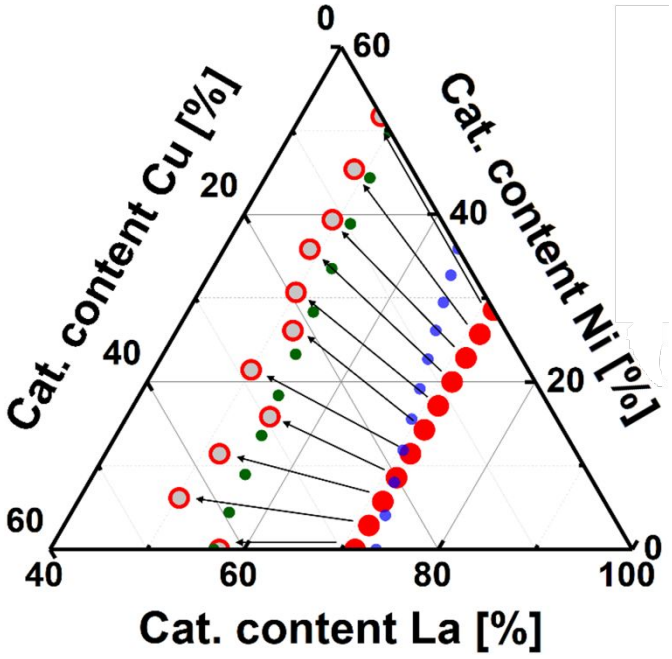

Figure 1: Pulsed cation concentration (filled red circles) and deposited cation concentration as measured by XRF (open red circles) in the La-Ni-Cu-O ALD process, deposited by substituting Ni(acac)2 with Cu(acac)2 in the recipe for LaNiO3. The black arrows show which deposited concentration corresponds to which pulsed concentration. The blue points correspond to the estimated deposited concentration given by the binary GPC model. The green points correspond to our estimated cation composition according to the ternary combination method.

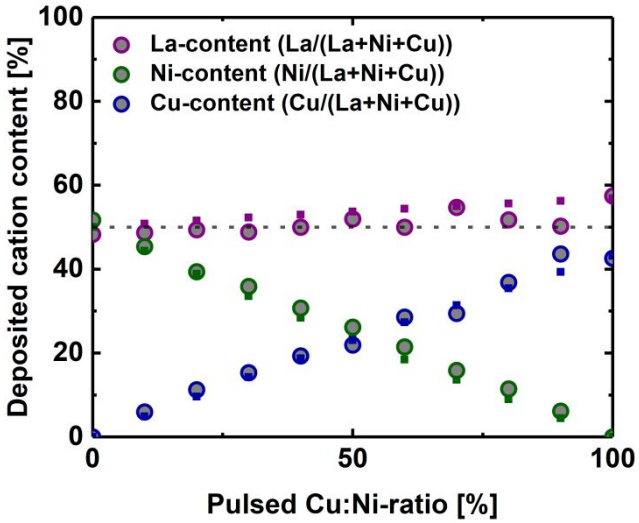

Figure 2. Deposited cation composition as a function of the ratio of the Cu:Ni pulsing ratio, as measured by XRF. The open circles correspond to the deposited ratios of La (purple), Ni (green) and Cu (blue) as measured by XRF. The dotted lines correspond to the predicted cation composition from the ternary combination method.

We observe that the La-content increases slightly with increased level of Cu substitution. This is predicted by the model, and is an expected result since it is likely that more $La(thd)_3$ pulses reacts with a Cu-O*-terminated surface, that previously has been shown to catalytically decompose metalorganic precursors and ozone.[21] We claim that we can control the $LaNi_{1-x}Cu_xO_{3-\delta}$ stoichiometry with high precision for $0 < x < 0.5$, but note that precision is reduced for $x > 0.5$. The obtained substitution range is substantially larger than what has been reported in bulk $LaNi_{1-x}Cu_xO_{3-\delta}$ ($x < 0.3$). [19]

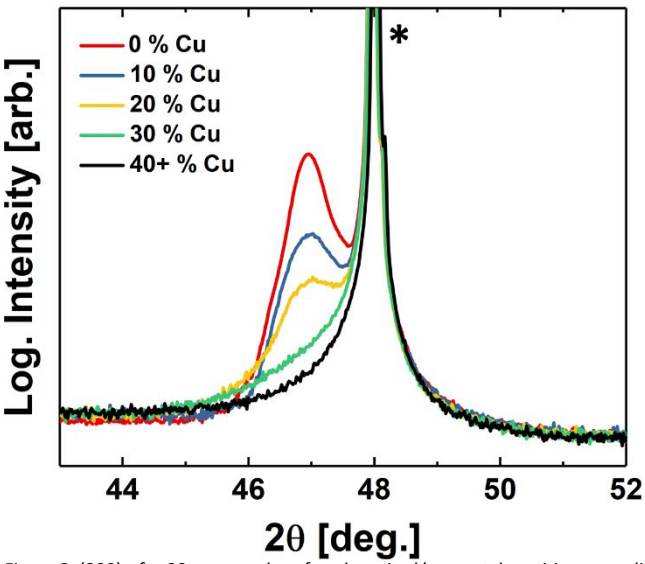

Figure 3. $(200)_{pc}$ for 30 nm samples of *as deposited* (no post deposition annealing) $LaNi_{1-x}Cu_xO_{3-\delta}$ on $LaAlO_3$ (100) , with five different substitution levels. The substrate (200) reflection is marked by *.

As deposited epitaxy of $LaNiO_3$ by ALD was recently reported.[21] Upon copper substitution in the $LaNiO_3$ process, we observe that the as-deposited oriented growth becomes less pronounced for increasing substitution amounts. Up to 30 % Cu-substitution, the films are crystalline and single-oriented as-deposited, albeit with lower quality going from pure $LaNiO_3$ to 30 % substitution (Figure 3). Above 30 % substitution there is no sign of as-deposited crystallinity for any of the samples.

Upon annealing at 650 °C for 15 minutes, all the films deposited on $LaAlO_3$ $(100)_{pc}$ substrates become crystalline and single-oriented (Figure 4). For substitution levels up to 50 %, the films are phase pure with only the perovskite phase present. Figure 4 also show how the lattice parameter increases upon increased Cu:Ni substitution, lowering the value of the (200) reflection maxima. This change can either be an effect of the incorporation of larger Cu^{2+} atoms at Ni^{3+}-sites, and/or an increased number of oxygen vacancies that naturally follows from this substitution. It has previously been shown that copper does not take a +III state under the conditions applied.[20] For substitution levels above 50 %, the obtained films are no longer phase pure, and contain an additional and varying amount of RP1. The presence of RP1 is believed to be an effect of increased nucleation probability for this phase on the $LaAlO_3$-surface. Epitaxial growth, as observed on $LaAlO_3$ $(100)_{pc}$ is likely to alter the growth of the binary constituents when compared to amorphous growth. It is also worthwhile to note that the samples with the highest amount of RP1 (70 and 100 % Cu) are slightly over-stoichiometric in La (53 and 57 %, respectively). This is likely also a significant cause for the formation of RP1.

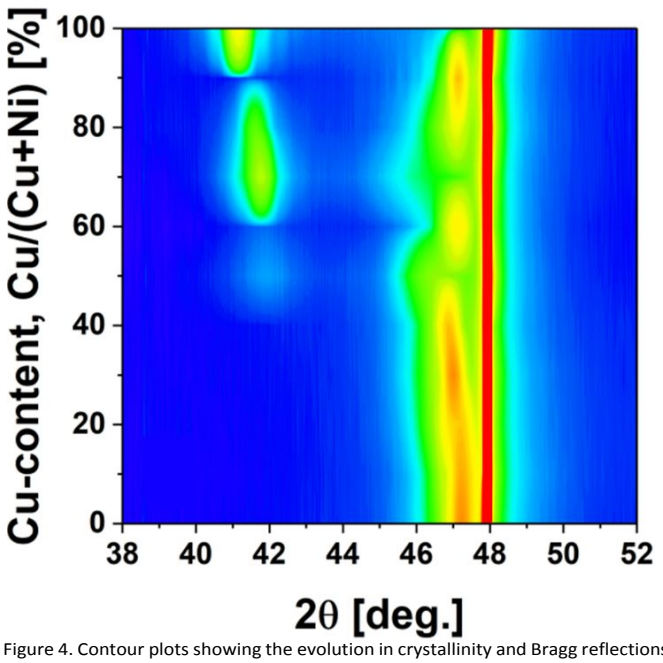

Figure 4. Contour plots showing the evolution in crystallinity and Bragg reflections for 30 nm thin films of $LaNi_{1-x}Cu_xO_{3-\delta}$ on $LaAlO_3$ $(100)_{pc}$ from x = 0.00 to x = 1.00 after post annealing at 650 °C for 15 minutes in air. The plot is constructed based on 11 diffractograms x, showing the full substitution space. Reflections for the RP1 (006) and the perovskite $(200)_{pc}$ are evident, as well as the substrate $(200)_{pc}$, shown as a hard red line.

To summarize the growth and the phase analysis, we have deposited films in the $LaNi_{1-x}Cu_xO_{3-\delta}$ system with high phase purity and compositional control up to 50 % Cu-substitution. At higher incorporated levels of Cu, decomposition effects from intermediary CuO*-surfaces makes such control challenging. RP1 seems to form easily on $LaAlO_3$ $(100)_{pc}$ substrates for slightly overstoichiometric La-compositions.

The chemical nature of the films was studied by soft x-ray absorption spectroscopy (XAS) of the Ni L- and Cu L-edges for films with different Cu-substitution levels (Figure 5). The Ni L-edge absorption corresponds to excitation from an occupied Ni 2*p* core state to an unoccupied Ni 3*d* state above the Fermi level, and is well suited for studying tunable electronic properties. The observed Ni L_3 signal is split in two, with a sharp multiplet at ~ 852 eV (A) and a broader multiplet at ~ 854 eV (B). The relative intensity distribution between these two peaks have previously been assigned to two effects: A gradual change in the oxidation state from Ni^{3+} to Ni^{2+}; and a change in the Ni 3*d* – O 2*p* hybridization strength. [27-29] For metallic $LaNiO_3$, a pure ionic model is certainly highly approximate at the best, furthermore, the ground state would then be composed of a mixture of $3d^7$, $3d^8\underline{L}$ and $3d^9\underline{L}^2$, where $\underline{L}$ denotes a ligand hole. Arguments have been made that the intensity distribution between these two peaks can be assigned to the degree of hybridization, and that an intense (A) is a result of weak hybridization.[27] The changes in properties due to both effects are nonetheless congruent: The relative reduction in the signal (A) reflects a situation with less conducting Ni-O-Ni interactions. The same changes are seen for $SmNiO_3$ when transitioning between its insulating to metallic states. [30] Pure $LaNiO_3$ films are highly metallic, nevertheless, a strong (A) peak is frequently reported due to oxygen vacancies that are likely to be present at the outer surface. It is interesting that Cu-substitution seems to enhance the metallic Ni-O-Ni bonding. This effect may possibly in the future be utilized to remove the current thickness limit for conduction in $LaNiO_3$, which is strongly suppressed by oxygen vacancies for ultra-thin films. [16] No qualitative change is observed in the Cu L-edge, showing that Cu is maintained in its +II state.

The room temperature electric properties of the films deposited on $LaAlO_3$ $(100)_{pc}$ were investigated by 4-point probe resistivity measurements (Figure 6). We measure a resistivity of ~120 μΩ cm for pure $LaNiO_3$. As the Cu-level increases, so does, expectedly, also the resistivity. For up to 80 % substitution, the resistivity increases smoothly towards ~100 mΩ cm. This could be due to decreasing crystallinity and/or an increase in oxygen vacancies due to Cu^{2+} substitution. For pure La-Cu-O, the resistivity dramatically increases to semiconducting/insulating levels, peaking at 100 Ω cm for 100 % substitution. Note that the resistivity can be tuned smoothly as function of composition over almost six orders of magnitude for as-deposited films.

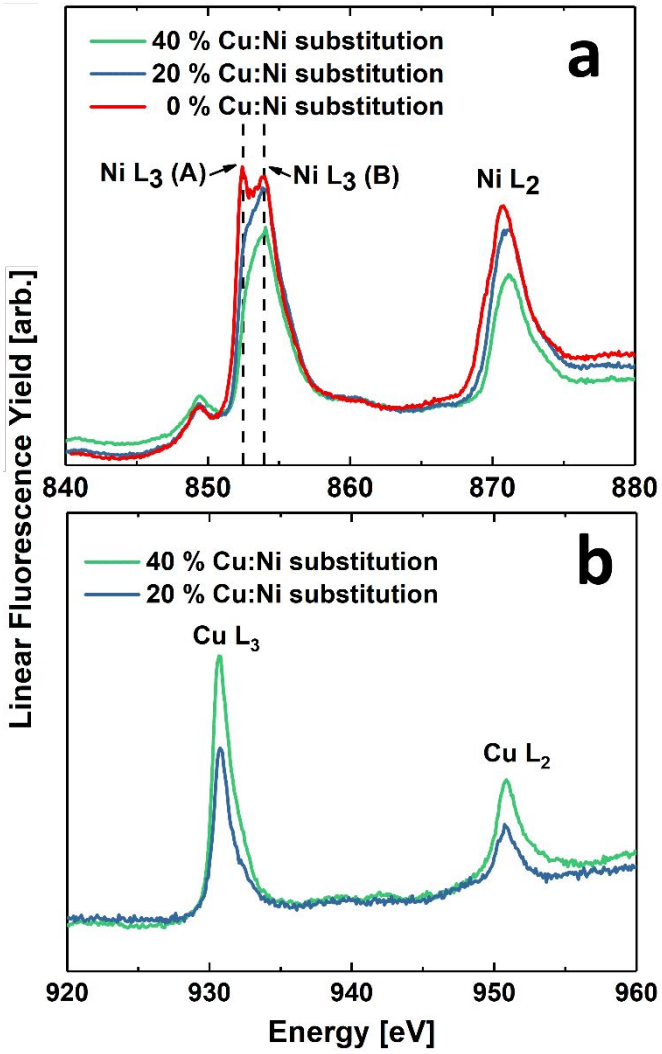

Figure 5. Soft x-ray absorption spectra of 30 nm thick $LaNi_{1-x}Cu_xO_{3-\delta}$ on $LaAlO_3$ (100) for (a) Ni L-edge and (b) Cu L-edge.

After annealing, the trend in resistivity remains, yet the variation is less pronounced. The resistivity is ~100 μΩ cm for pure $LaNiO_3$, and is maintained at a low level (< 500 μΩ cm), increasing slowly for $x < 0.40$. The variation gets more pronounced for > 50 % Cu-substitution, with a general trend of increased resistivity at higher Cu-substitution levels. The anomalies in resistivity for some samples correspond to films containing some RP1. This shows that both crystallinity and phase purity of the perovskite phase, in addition to Cu-substitution level, are important for the electronic transport properties.

Although the measured specific resistivity provides a reasonable input to understanding the electronic behavior of a material (*i.e.* metallic, semiconducting or insulating), a temperature dependent resistivity study gives more insight into the transport mechanisms. We studied the temperature dependence of the resistivity for samples deposited on $LaAlO_3$ $(100)_{pc}$ in order to identify the transport characteristics of the films and the existence of any MIT (Figure 7).

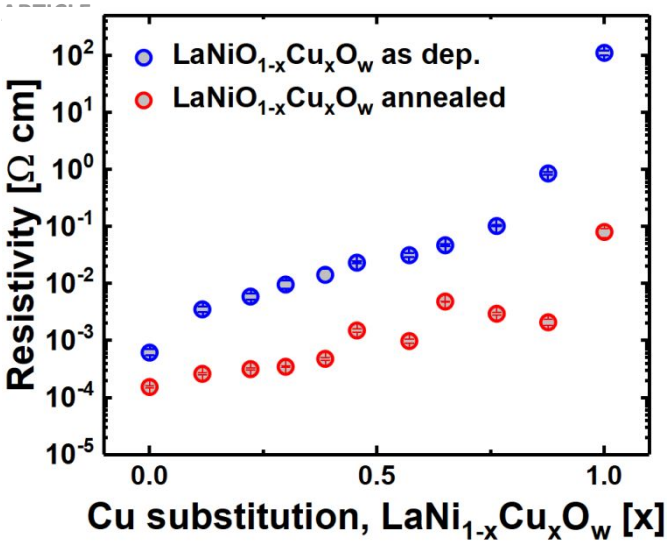

Figure 6. Room temperature resistivity as a function of Cu-substitution for 30 nm $LaNi_{1-x}Cu_xO_{3-\delta}$ thin films deposited on $LaAlO_3$ $(100)_{pc}$. Blue circles correspond to as-deposited samples, red circles correspond to samples annealed at 650 °C in air for 15 minutes.

Pure $LaNiO_3$ is a metal at all temperatures, and so are the films

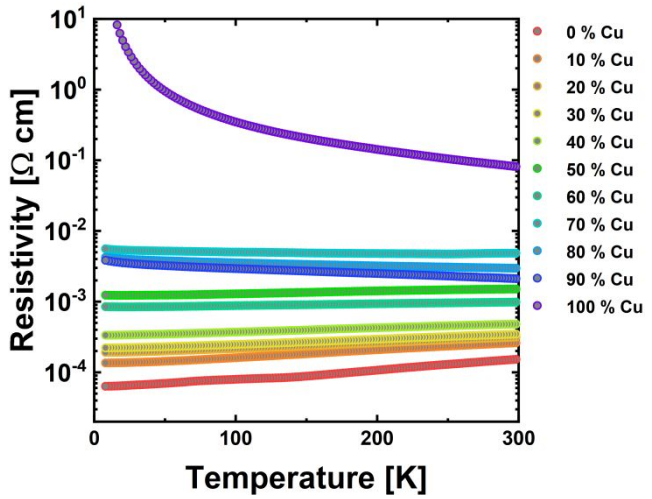

with 10 and 20 % Cu- substitution. For 30 % Cu-substitution we observe a weak signature of an MIT just below 10 K, very similar to what is seen in ultrathin $LaNiO_3$.[31] For 40, 50 and 60 % Cu-substitution, the MIT temperature steadily increases to 12, 22 and 29 K, respectively. Note that the change in resistivity for the sample with composition $LaNi_{0.4}Cu_{0.6}O_{3-\delta}$ is only 15 % over the whole temperature range. This shows how tuning the electronic properties by B-site substitution can enable materials with extremely low thermal coefficient values. For 70 % Cu-incorporation, a jump to 245 K is observed, while for 80 % incorporation we cannot determine a stringent MIT, although the temperature dependence of the resistivity is flat around room temperature. The 90 and 100 % Cu-incorporated samples are semiconducting/insulating at room temperature.

Figure 7. Resistivity as a function of temperature for 30 nm $LaNi_{1-x}Cu_xO_{3-\delta}$, $0.0 < x < 1.0$ thin films deposited on $LaAlO_3$ $(100)_{pc}$. Note logarithmic scale on the y-axis.

Figure 8 summarizes the trends in MIT across the whole substitution range. The MIT temperature is taken at (dp/dT = 0) (see Electronic Supporting Information for detailed linear plots).

Note that the MIT temperature does not seem to be correlated to the crystalline quality as much as the specific resistivity, *e.g.* for the 70 % Cu-incorporated sample. This fits well with the MIT being an inherent physical property governed by band splitting, and that it (in theory) should not change due to *e.g.* a large number of grain boundaries. The MIT temperature varies from 0 K for $LaNiO_3$ to above room temperature for highly Cu-substituted samples. A more careful study of the substitution between 60 and 70 % Cu-levels is necessary to gain further insight to the variation of the MIT temperature above 30 K.

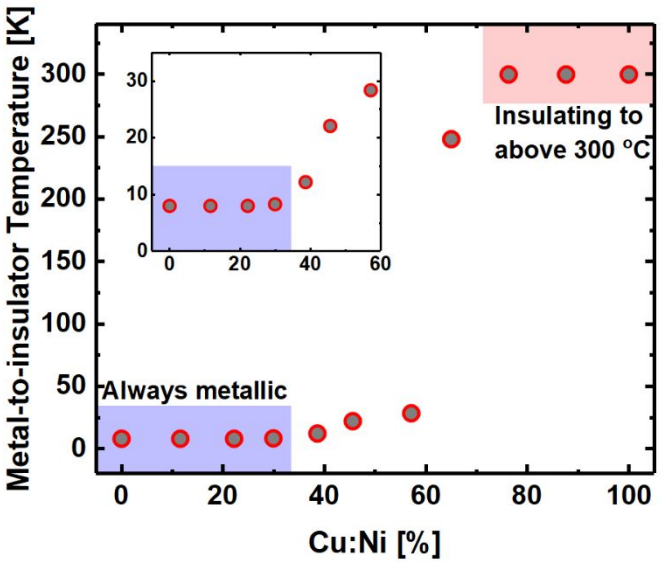

Figure 8. Metal-to-insulator transition temperature as a function of Cu:Ni substitution for 30 nm $LaNi_{1-x}Cu_xO_{3-\delta}$ thin films deposited on $LaAlO_3$ $(100)_{pc}$, for $0 < x < 1$. The transition temperature is taken at dp/dT = 0.

Conclusions

In this work we have deposited thin films of $LaNi_{1-x}Cu_xO_{3-\delta}$ across the whole substitution range ($0.0 < x < 1.0$) by means of ALD. The attainable substitution range is found to be much larger than what has previously been reported for bulk samples. The films grow single oriented out of plane on $LaAlO_3$ $(100)_{pc}$ for low substitution levels ($x < 0.4$), but are amorphous as-deposited for higher Cu-contents. The higher Cu-content amorphous films on $LaAlO_3$ $(100)_{pc}$ can be crystallized upon annealing at 650 °C in air, however, high Cu-content films have a tendency to co-form an RP1 phase in conjunction with the perovskite phase. The chemical nature of the films is dominated by Ni^{3+} and Cu^{2+} as measured by XAS. The Cu-substitution seems to remove any Ni^{2+} signature in the films.

We studied the electrical properties by means of 4-point probe measurements, revealing that the resistivity is affected by the level of Cu-substitution as well as phase purity and level of crystallization. We hypothesize that the diminishing

conductivity on increasing Cu-content results from a reduction in the Ni(Cu)-O-Ni(Cu) bond angle as well by oxygen vacancies needed to maintain an average oxidation state of +II for copper. We note that this material system can be used to obtain thin films with highly controllable and variable resistivity, spanning six orders of magnitude on $LaAlO_3$ $(100)_{pc}$ substrates. Films with very low (< 15 %) temperature variation are also attainable. This variable resistivity control could in the future prove to become essential in the design of novel complex oxide electronic devices.

Conflicts of interest

There are no conflicts to declare.

Acknowledgements

This work was carried out within the RIDSEM project, financed in full by the Research Council of Norway (project number 272253). The Research Council of Norway is also acknowledged for the support to the Norwegian Center for x-ray Diffraction, Scattering and Imaging (RECX). We would furthermore like to acknowledge Dr. Susmit Kumar for assistance with the PPMS infrastructure. The x-ray absorption spectroscopy work was carried out at the Advanced Photon Source, Argonne National Laboratory, supported by the U.S. Department of Energy, Office of Science under Grant No. DEAC02-06CH11357.

Notes and references

1 M. Coll, J. Fontcuberta, M. Althammer, M. Bibes, H. Boschker, A. Calleja, G. Cheng, M. Cuoco, R. Dittmann, B. Dkhil, I. El Baggari, M. Fanciulli, I. Fina, W. Fortunato, C. Frontera, S. Fujita, V. Garcia, S. T. B. Goennenwein, C. G. Granqvist, J. Grollier, R. Gross, A. Hagfeldt, G. Herranz, K. Hono, E. Houwman, M. Huijben, A. Kalaboukhov, D. J. Keeble, G. Koster, L. F. Kourkoutis, J. Levy, M. Lira-Cantu, J. L. MacManus-Driscoll, J. Mannhart, R. Martins, S. Menzel, T. Mikolajick, M. Napari, M. D. Nguyen, G. Niklasson, C. Paillard, S. Panigrahi, G. Rijnders, F. Sánchez, P. Sanchis, S. Sanna, D. G. Schlom, U. Schroeder, M. Spreitzer, J. van den Brink and F. Miletto Granozio, *Appl. Surf. Sci.*, 2019, **482**, 1.
2 P. Yu, Y.-H. Chu, R. Ramesh, *Mater. Today*, 2012, **15**, 320.
3 L. Bjaalie, B. Himmetoglu, L. Weston, A. Janotti and C. G. van de Walle, *New J. Phys.*, 2014, **16**, 025005.
4 A. Ohtomo and H. Y. Hwang, *Nature*, 2004, **427**, 423.
5 J. Torrance, P. Lacorre, A. Nazzal, E. Ansaldo and C. Niedermayer, *Phys. Rev. B*, 1992, **45**, 8209.
6 J. A. Alonso, M. J. Martínez-Lope, M. T. Casais, J. L. García-Muñoz and M. T. Fernández-Diaz, *Phys. Rev. B*, 2000, **61**, 1756.
7 G. Catalan, *Phase Transit.* 2008, **81**, 729.
8 J. A. Alonso, M. J. Martínez-Lope, M. T. Casais, M. A. G. Aranda and M. T. Fernández-Diaz, *J. Am. Chem. Soc.*, 1999, **121**, 4754.
9 N. Hamada, *J. Phys. Chem. Solids* 1993, **54**, 1157.
10 M. L. Medarde, *J. Phys. Condens. Mat.*, 1997, **9**, 1679.
11 S. R. Barman, A. Chainani and D. D. Sarma, *Phys. Rev. B* 1994, **49**, 8475.
12 S. Catalano, M. Gibert, J. Fowlie, J. Íñiguez, J. M. Triscone and J. Kreisel, *Rep. Prog. Phys*., 2018, **81**, 046501.
13 P. Ganguly, N. Y. Vasanthacharya, C. N. R. Rao and P. P. Edwards, *J. Solid State Chem.*, 1984, **54**, 400.
14 C. N. R. Rao, O. M. Parkash and P. Ganguly, *J. Solid State Chem.*, 1975, **15**, 186.
15 D. Misra and T. K. Kundu, *Mater. Res. Express*, 2016, **3**, 095701.
16 I. C. Tung, G. Luo, J. H. Lee, S. H. Chang, J. Moyer, H. Hong, M. J. Bedzyk, H. Zhou, D. Morgan, D. D. Fong and J. W. Freeland, *Phys. Rev. Mater.*, 2017, **1**, 053404.
17 B. Normand and T. M. Rice, *Phys. Rev. B*, 1996, **54**, 7180.
18 I. Álvarez, M. L. Veiga and C. Pico, *J. Solid State Chem*., 1998, **136**, 313.
19 G. R. Moradi, F. Khosravian and M. Rahmanzadeh, *Chinese J. Catal.*, 2012, **33**, 797.
20 H. H. Sønsteby, J. E. Bratvold, K. Weibye, H. Fjellvåg and O. Nilsen, *Chem. Mater.*, 2018, **30**, 1095.
21 H. H. Sønsteby, E. Skaar, Ø. Fjellvåg, J. E. Bratvold, H. Fjellvåg and O. Nilsen, *Nat. Commun.* 2020, **11**, 2872.
22 M. D. McDaniel, T. Q. Ngo, S. Hu, A. Posadas, A. A. Demkov, and J. G. Ekerdt, *Appl. Phys. Rev.* 2015, **2**, 041301.
23 H. H. Sønsteby, H. Fjellvåg and O. Nilsen, *Adv. Mater. Interfac.* 2017, **4**, 1600903.
24 A. J. M. Mackus, J. R. Schneider, C. Macisaac, J. G. Baker and S. F. Bent, *Chem. Mater.* 2019, **31**, 1142.
25 M. Lie, O. Nilsen, H. Fjellvåg, and A. Kjekshus, *Dalton T.* 2009, 481.
26 O. Nilsen, E. Rauwel, H. Fjellvåg, H, A. Kjekshus, *J. Mater. Chem.* 2007, **17**, 1466.
27 C. Piamonteze, F. M. F de Groot, H. C. N. Tolentino, A. Y. Ramos, N. E. Massa, J. A. Alonso and M. J. Martínez-Lope, *Phys Rev. B* 2005, **71**, 020406.
28 M. Medarde, A. Fontaine, J. L. García-Muñoz, J. Rodríguez-Carvajal, M. de Santis M. Sacchi, G. Rossi and P. Lacorre, *Phys. Rev. B* 1992, **46**, 14975.
29 J. W. Freeland, M. van Veenendaal and M. Chakhalian, *J. Electron. Spectrosc.* 2016, **208**, 56.
30 F. Y. Bruno, S. Valencia, R. Abrudan, Y. Dumont, C. Carrétéro, M. Bibes, A. Barthélémy, *Appl. Phys. Lett.* 2014, **104**, 021920.
31 M. Golalikhani, Q. Lei, R. U. Chandrasena, L. Kasaei, H. Park, J. Bai, P. Orgiani, J. Ciston, G. E. Sterbinsky, D. A. Arena, P. Shafer, E. Arenholz, B. A. Davidson, A. J. Millis, A. X. Gray and X. X. Xi, *Nat. Commun.* 2018, **9**, 2206.

TOC Entry for "Tuning Electronic Properties in $LaNiO_3$ Thin Films by B-site Cu-substitution" – Sønsteby *et al.*

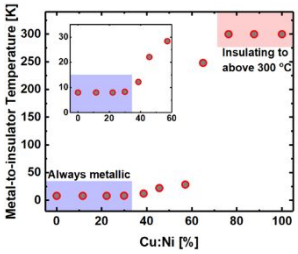

Cu-substitution in $LaNiO_3$ by atomic layer deposition provides films spanning six orders of magnitude in resistivity, with metal insulator transition temperatures from 0 K to room temperature.